Immunoinformatics Approaches for Developing Multi-Epitope Subunit Vaccines to Combat Acinetobacter Baumannii

Pinhua Pan (pinhuapan668@csu.edu.cn)
Xiangya Hospital Central South University https://orcid.org/0000-0001-5883-0531
Fei Zhu
Xiangya Hospital Central South University
Shiyang Ma
Xiangya Hospital Central South University
Mingjun Rao
Xiangya Hospital Central South University
Peipei Zhang
Xiangya Hospital Central South University
Wenzhong Peng
Xiangya Hospital Central South University
Yanhui Cui
Xiangya Hospital Central South University
Hang Yang
Xiangya Hospital Central South University
Caixia Tan
Xiangya Hospital Central South University
Jie Chen
Xiangya Hospital Central South University

Original article

Keywords: Acinetobacter baumannii, multiepitope vaccine, molecular docking, molecular dynamics, informaticimmunology

Posted Date: January 25th, 2022

DOI: https://doi.org/10.21203/rs.3.rs-1249947/v1

Abstract

Acinetobacter baumannii, a Gram-negative opportunistic pathogen that widely exists in the environment, causes numerous nosocomial infection cases in the ICU. As the agent of pneumonia, septicemia, and meningitis, *A. baumannii* is usually multidrug-resistant and has a high mortality rate. In this study, we aimed to develop a vaccine for *Acinetobacter baumannii* through in silico prediction. With the help of immunoinformatic methods, which have proven to be effective and convenient, our team managed to develop multiepitope subunit vaccines for *A. baumannii*. Three proteins closely associated with the immunologic process were selected and computed. Finally, 9 cytotoxic T-lymphocyte (CTL) epitopes, 10 helper T-lymphocyte (HTL) epitopes, and 11 linear B cell (LBL) epitopes were selected to construct 2 vaccines. LT-IIb was selected as an adjuvant and attached to the vaccine N-terminus. All subunits are linked by suitable linkers. According to examinations, both MEV is antigenic and stable without poisonousness or allergenicity. Molecular docking revealed steady and solid binding ability between MEV and Toll-like receptors (TLRs) and the major histocompatibility complex (MHC). Finally, MEV codons were optimized into a plasmid for in silico cloning, which is pet-28a+ from *E. coli K-12* in this research. Although this vaccine performed well in immune stimulation, further experiments are expected to guarantee its safety and immunogenic profile.

Key Points

1. Select epitope to develop 2 vaccines **2.** Verify their validity in informatic method

Introduction

ESKAPE comprises 6 first letters from 6 microscopic organisms, *E. faecium*, *S. aureus*, *K. pneumonia*, *A. baumannii*, *P. aeruginosa*, and *Enterobacter* species. These bacteria managed to escape from mostly existing antibacterial agents and will long last turn into an approaching looming threat to human health(De Oliveira et al. 2020). Described as a successful pathogen, *A. baumannii* is ubiquitous in the environment from soil to water(Peleg et al. 2008) and can colonize the skin, respiratory tracks, and wounds. Usually, it causes infection in debilitated patients(Munoz-Price and Weinstein 2008) and leads to clinical manifestations such as ventilator-associated pneumonia (VAP), blood infectious, respiratory, urinary, or gastrointestinal tract infections, and sepsis-associated with long-term device use(Nasr 2020). What turned *A. baumannii* into an urgent threat is resistance to multiple antibiotics, especially carbapenems(Ramirez et al. 2020), and the resistance mechanisms that *A. baumannii* has achieved consist of β-lactamases, aminoglycoside-modifying enzymes, permeability defects, efflux pumps, and target site modifications(Kyriakidis et al. 2021; Lee et al. 2017). The infection of *A. baumannii* has caused great damage to public health worldwide, and the prevalence of infection could be 2%-4% among all medical-related infections and over 10% in the ICU(Lotsch et al. 2020; Ma and McClean 2021; Meng et al. 2021). A total of 1011 strains collected from 48 countries show that more than half of the strains are multidrug-resistant (MDR)(Lob et al. 2016); unfortunately, it is estimated that the mortality of MDR *baumannii* is more than 50%(Ma and McClean 2021). Accordingly, strategies unrelated to antibiotics are needed due to the absence of significant agents. Vaccines, for instance.

In the previous decade, numerous strategies have been examined for pursuing an efficient vaccine, including whole-cell vaccines, subunit vaccines, multicomponent vaccines, and nucleic acid vaccines; however, none of them finally stepped into a clinical study, and these studies revealed a possible future(Gellings et al. 2020; Ma and McClean 2021). Traditional vaccine development is mainly based on experience and consumes much time and labor, but with the favor of developing immunoinformatic methods, in silco vaccine design can be a new trend(He et al. 2010). To date, attempts to develop a vaccine for different pathogens, including bacteria, viruses, parasites or even tumors, have been made(Oli et al. 2020), among which most are about COVID-19. What immunoinformatic methodologies can do covers epitope prediction, vaccine design, and analysis of molecular docking. Multiepitope vaccines designed by in silco methods have induced strong immunoreactions against acute *Toxoplasma gondii*-infected(Foroutan et al. 2020) and *Trichinella spiralis*-infected mice(Gu et al. 2017), while B cell epitope vaccine-induced IgG1 protective responses against *MRSA*-infected mice(Zhao et al. 2015). It is feasible and effective to design vaccines through immunoinformatics.

Building vaccines based on epitope selection is a strategy with solid evidence. The core of protective immunity is T lymphocytes. The antigen segment is presented to the MHC protein and activates T cells. MHC II triggers helper T cells, while MHC I trigger cytotoxic T cells. After receiving information from MHC molecules, T cells activate the growth and differentiation of B lymphocytes and finally produce protective antibodies. By directly predicting epitopes that can combine with antigen-binding grooves according to different MHC alleles, we can search pathogen protein sequences and find epitopes that hopefully cause a protective immune response. The

prediction of T cell epitopes has been mentioned(Moise and De Groot 2006) and confirmed valid(Lundegaard et al. 2006), but informatic vaccine design did not receive enough attention until an urgent need for a new vaccine in the pandemic of *coronavirus 2019*(Sohail et al.). Informative immunology has been developed greatly in the past decade. A recent study revealed that more than 95% of T cell epitopes obtained from experiments can be predicted by at least one in silco method(Sohail et al.), which is an inspiring result for vaccine development. Forming predicted epitopes into multiepitope vaccines is a convenient way of developing vaccines. Compared with a monovalent vaccine, MEV is believed to elicit a variety of human immune responses(Amanna and Slifka) since it contains more epitopes to activate immunocytes. In theory, LBL epitopes can directly activate B lymphocytes, although more studies are needed, combining LBL epitopes with T cell epitopes may enhance the protection of vaccines(Grandi et al.).

In this study, Outer membrane protein A (OmpA), Outer membrane W (OmpW), and Outer membrane protein33-36 (Omp33-36) were selected for additional prediction of CTL, HLT, and LBL epitopes according to MHC alleles. These epitopes were analyzed by their antigenicity, toxicity, and allergenicity, and epitopes with better performance were selected for our final MEV. Finally, two multiepitope vaccines were designed, one containing the epitopes of OmpA and Omp33-36 and the other containing the epitopes of OmpA and OmpW, to compare the efficiency of different matches.

Materials And Methods

Amino acid sequence retrieval

Fasta files containing sequence information of *Acinetobacter baumannii* OmpA (WP_000777878.1), OmpW (WP_004736587.1), and Omp33-36 (WP_000733005.1) were acquired from NCBI (https://www.ncbi.nlm.nih.gov/). Similarly, the amino acid sequence of LTIIb (PDB: 5G3L_H) was acquired from NCBI.

Prediction and selection of CTL epitopes

Cytotoxic T-lymphocyte (CTL) epitopes were predicted from OmpA, OmpW, and Omp33–36 sequences through the NetCTL server version 1.2, which has been shown to have exceptional predictive performance(Larsen et al.). The epitopes of all supertypes in the server were identified at a combined score of 0.75. The Vaxijen2.0 server was utilized to examine the peptides' antigenic potential through the physical and chemical properties of amino acid sequences, with an accuracy of between 70% and 89%(Doytchinova and Flower). A threshold value of 0.5 was considered. Furthermore, the antigenic epitopes (value>0.5) were predicted for their immunogenicity via the IEDB program (http://tools.iedb.org/immunogenicity/)(Calis et al.) The Toxinpred server (https://webs.iiitd.edu.in/raghava/toxinpred/index.html) was used to check for epitopic toxicity and their physicochemical properties(Gupta et al.). Epitopic allergenicity was predicted through the AllerTOP 2.0 (https://www.ddg-pharmfac.net/AllerTOP/index.html) server(Wold. et al.). The consensus algorithm was chosen to predict MHC I allelic partners of the screened epitopes via Tepitool (http://tools.iedb.org/tepitool/)(Paul et al.). The percentile rank score ≤ 2 and inhibitory concentration (IC50) <500 nM mean that peptides have a decent fondness to the receptor, which were under consideration.

Prediction and selection of HTL epitopes

The NetMHCIIpan 4.0 server (http://www.cbs.dtu.dk/services/NetMHCIIpan/) was utilized for predicting Helper T-lymphocyte epitopes, which have higher predictive performance for CD4 epitopes than the previous version(Reynisson et al.). A total of 14 human leukocyte antigen (HLA)DR alleles were chosen to cover as much of the world's population as possible for the prediction of MHC-II binding peptide epitopes, including DRB1*01:01; DRB1*03:01; DRB1*04:01; DRB1*04:04; DRB1*04:05; DRB1*07:01; DRB1*08:02; DRB1*09:01; DRB1*11:01; DRB1*13:02; DRB1*15:01; DRB3*01:01; DRB4*01:01; and DRB5*01:01(Wang et al.). The HTL epitopes were screened based on percentile rank score≤2 and inhibitory concentration (IC50) <500 nM. The antigenic capability of HTL epitopes was evaluated through Vaxijen2.0 at the threshold value of 0.5. Then, we used Toxinpred and AllerTOP 2.0 servers to check for epitopic toxicity and allergenicity. Cytokines are produced by HTL cells, such as IL-4, IL-12, and IFN-γ. IFN-γ is essential for the development of Th1 cells(Ivashkiv), while IL-4 is involved in the regulation of Th2 differentiation(Steinke and Borish). Based on the motif scan and SVM hybrid approaches, INF-γ-inducing epitopes were screened out through the INFepitope server (https://webs.iiitd.edu.in/raghava/ifnepitope/design.php)(Dhanda et al.). IL-4-inducing HTL epitopes were predicted through the IL-4pred server (https://webs.iiitd.edu.in/raghava/il4pred/design.php) (Dhanda et al.).

Prediction and screening of LBL epitopes

The ABCpred server (https://webs.iiitd.edu.in/raghava/abcpred/) utilizes the trained recurrent neural network for predicting linear B cell epitopes at 65.93% accuracy. At a length of 16 and threshold of 0.8, we predicted B epitopes(Saha and Raghava). The antigenic potential of B cell epitopes was evaluated through Vaxijen2.0 at the threshold value of 0.5. Epitopic toxicity and allergenicity were predicted by the Toxinpred and AllerTOP 2.0 servers.

Assessment of epitope homology with human proteins

Blast (https://blast.ncbi.nlm.nih.gov/Blast.cgi) was utilized to detect the homology between epitopes and human proteins to reduce the occurrence of cross-reactivity and autoimmune diseases.

Design of Muti-epitope subunit vaccine

The most ideal epitopes chosen after an extensive screen were utilized to form multiepitope vaccines. Vaccine constructor 1 comprises epitopes of OmpA and Omp33-36, and vaccine constructor 2 consists of epitopes of OmpA and OmpW. The KK linkers were utilized to connect CTL and HTL epitopes, which are identified with the antigenic peptidase digestion site presented by cathepsin B to T cells(Takahashi et al. 1989). B cell epitopes were linked by GPGPG linkers, which are notable adaptable linkers(Yousafi et al. 2021). LT-IIb was considered to be a suitable adjuvant attached to the N-terminus of vaccines, which could improve the immunogenicity of the designed vaccine. Proper linkers can help stabilize the protein structure; for instance, the linker between adjuvant and vaccine is the EAAAK sequence(Nezafat et al. 2014). The designed vaccines' physicochemical characteristics were estimated through the ProtParam server (https://web.expasy.org/protparam/) (Wilkins et al. 1999). There are many physicochemical properties of the vaccine, among which the more important ones are molecular weight, theoretical pI, half-life, instability index, aliphatic index, and grand average of hydropathicity (GRAVY). When the shakiness file is under 40, it proposes that the protein is steady(Guruprasad et al. 1990).

The SQLpro server (http://scratch.proteomics.ics.uci.edu/) was utilized to check for the overpressed protein solubility in *E. coli* with a general exactness of more than 74%(Magnan et al. 2009). The vaccine's immunogenicity was affirmed through the Vaxijen2.0 server and ANTIGENpro server (http://scratch.proteomics.ics.uci.edu/), and lastone has been proven to be an accurate server with an accuracy of over 70%(Magnan et al. 2010). Two vaccines' allergenicity was determined through two distinct servers, AlgPred2.0 and AllerTOP v2.0.

Secondary structure prediction

Prabi (https://npsa-prabi.ibcp.fr/cgi-bin/npsa_automat.pl?page=/NPSA/npsa_gor4.html) was used to predict the secondary structure of designed vaccines based on the GOR4 method with a precision of 64.4%(Garnier et al.)

Modeling and validation of vaccine

The designed vaccine was a reconstituted protein without detectable homology except for the added adjuvant, and its 3D model was generated through the RaptorX server (http://raptorx.uchicago.edu/). This server predicted 3D structures of the protein sequence through deep convolutional residual neural networks (ResNet)(Xu et al.). Recent reports have shown that RaptorX servers perform better and have higher accuracy in predicting human-designed proteins(Wang et al. 2017; Xu 2019). Then, we utilized the Galaxy server (http://galaxy.seoklab.org/) to refine the vaccine structure, which was based on the ab initio method(Ko et al.). The Galaxy refine server generated five different refined models of the designed vaccine. The main 3 parameters of this server, GDT-HA, RMSD, and MolProbity, were used to assess the models. To verify the quality of the selected model, the models were evaluated via ERRAT, PROCHECK, and ProSA servers. ERRAT evaluated our models based on the nonbonded atomic interactions of the various atomic types within the protein. The ProSA website (https://prosa.services.came.sbg.ac.at/prosa.php) evaluated the overall quality and generated a Z score(Wiederstein and Sippl). A positive Z score implies that there might be mistakes in the protein model.

Immune Simulations

To evaluate the immunogenic features of the designed vaccine, we subjected its sequence to C-ImmSim (https://kraken.iac.rm.cnr.it/C-IMMSIM/index.php?page=0), an immune response prediction server(Rapin et al.). This server evaluates the host immune response toward antigens by a position-specific scoring matrix (PSSM). For immune stimulation, a total of three injections with an interval of 4 weeks were used to activate the simulated immune system, and the parameter containing vaccines was 1000 units for each. The step number in the immune simulation process was 1050, each time step represented 8 hours, and the time steps of the three injections were set at 1, 84, and 168. Other parameters were default.

Molecular docking

The designed vaccine ought to have a high binding proclivity to immune-related receptors, such as MHC molecular and Toll-like receptors, to trigger an appropriate immune response. TLR2 plays a significant role in the host's innate immune response to microbial infection, while TLR4 is likewise important in the clearance of *Acinetobacter baumannii* and the induction of proinflammatory cytokines and chemokines(March et al.). Molecular docking is an informatic method to assess the interaction between two kinds of moleculars' crystal structure complex of human TLR4(PDB ID:4G8A), TLR2(PDB ID:2Z7X), MHC I molecular (PDB ID:1X7Q), MHC II molecular (PDB ID:5JLZ) and B cell receptor (PDB ID:3KG5) were obtained from the protein database bank. Then, the HADDOCK v2.4 server (https://wenmr.science.uu.nl/haddock2.4/) was used to evaluate the interactions between the designed vaccine and TLR2, TLR4, MHCI, MHCII, and BCR(van Zundert et al.). As a Forerunner in the molecular docking field from the WeNMR-EOSC Ecosystem, it provides a high-quality in-cloud integrative docking service(Honorato et al.). Then, better outcomes were submitted to the HADDOCK server for refinement. Furthermore, the PDBsum(http://www.ebi.ac.uk/pdbsum.) is utilized to analyze the interface of the refined complexes(Laskowski et al.) and Gibbs free energy predicted with PRODIGY, which can reflect the binding affinity of the complex(Xue et al. 2016).

Molecular Dynamic simulation

To further analyze the stability of the docked complex, we used the iMOD server (http://imods.chaconlab.org/). Based on normal mode analysis (NMA), iMODs are an intuitive server to simulate marcomolecule conformational changes in a natural and effective method (Lopez-Blanco et al. 2014). With the help of iMODs, we are able to measure the internal motions in the vaccine-receptor complex.

Population Coverage Analysis

There are differences in the distribution and expression of various HLA alleles across the globe's ethnic groups. The HLA allele distribution is vital for multiepitope vaccine constructs. The population coverage was calculated by the IEDB tool (http://tools.iedb.org/population/) through screening antigen epitopes according to HLA alleles(Bui et al.).

In silico cloning

The JCAT online server (http://jcat.de/) was used to back translate and optimize the condon of the vaccine(Grote et al.). Submitting the vaccine sequences to the JCAT server, the selected vector was pET28a+ from *E. Coli* (K12 strains). The two parameters of the JCAT severe, codon adaptive index (CAI), and GC content, play an important role in the evaluation of protein expression. Then, *Bam*HI restriction was added to the N-terminus and *Xho*I restriction was added to the C-terminus of the target sequence. The final step was to insert the sequence inside the vectors using SnapGene software. Figure 1 **here**.

Results

Prediction and selection of epitopes

44 CTL, 158HTL, and 36 LBL epitopes were obtained. These epitopes were further screened through numerous immune filters. For example, the epitopes used to construct vaccines should be nonallergenic, nontoxic should have high antigenicity and high affinity with HLA alleles. To make the multiepitope vaccine have higher antigenicity, only epitopes with high antigenicity scores are used to construct the vaccine. Finally, 7 CTL, 6 HTL, and 8 LBL epitopes were obtained to construct the vaccine. Complete epitope screening data can be found in the supplemental materials (Table S1, S2 and S3). Table 1 **here**, Table 2 **here**, Table 3 **here.**

Table 1
Final CTL epitopes selected for vaccine construction

Protein	Supertype	Start Position	Epitope Sequence	Score	Immunogenicity	Antigenicity	Allergic	Toxicity	Similarity with human protein
OmpA	A1	269	HTDNTGPRK	1.046	0.09127	1.6471	-	-	0
	B7	18	AANAGVTV	0.9721	0.13371	1.1461	-	-	
Omp33-36	A2	16	GAHAYQFEV	1.0009	0.09453	1.7241	-	-	0
		100	YVPTPYLPV	0.9688	0.00534	1.5876	-	-	0
		140	AMLLPNFLM	0.8631	0.06067	1.7425	-	-	0
OmpW	A1	308	FTAGFTYDF	1.5173	0.20718	1.267	-	-	0
	A2	160	FIGGIPPKV	1.1644	0.0289	1.4031	-	-	0

Table 2
Final HTL epitopes selected for vaccine construction

Protein	MHC Allele	Start Position	Epitope Sequence	Antigenicity	Allergic	Toxicity	IFN-γpred	IL-4pred	Similarity with human protein
OmpA	DRB1_0401	130	YKYDFDGVNRGTRGT	1.3463	-	-	+	+	0
	DRB3_0101								
	DRB1_1501	66	GIELTPWLGFEAEYN	0.9127	-	-	+	+	0
Omp33-36	DRB3_0202	233	VGATFVGNDGEADIK	0.9694	-	-	+	+	0
	DRB3_0202	235	ATFVGNDGEADIKGN	1.0696	-	-	+	+	0
OmpW	DRB1_0401	114	KPEVAGEATIQGLEQ	0.7934	-	-	+	+	0
	DRB1_0404								
	DRB1_1501	234	KSGVNKFRPYLGVGL	0.7925	-	-	+	+	0

Table 3
Final LBL epitopes selected for vaccine construction

Protein	Start Position	Epitope Sequence	Score	Antigenicity	Allergic	Toxicity	Similarity with human protein
OmpA	142	RGTSEEGTLGNAGVGA	0.94	1.8663	-	-	0
	83	KGDVDGASAGAEYKQK	0.86	1.9423	-	-	0
	42	NGGKDGNLTNAPELQD	0.82	1.5997	-	-	0
Omp33-36	259	YPNATARIEGHTDNTG	0.8	1.1391	-	-	0
	110	ASATYNHTDVDGKNNF	0.89	1.1803	-	-	0
	116	HTDVDGKNNFSKDDNG	0.88	1.6333	-	-	0
	87	NYHIGTYGVKGEAYVP	0.83	1.0537	-	-	0
OmpW	278	DGKAGAALDRKESSGN	0.87	1.8311	-	-	0
	234	KSGVNKFRPYLGVGL	0.84	0.7925	-	-	0

Multiepitope vaccine construction

The final multiepitope vaccines are composed of four parts: LT-IIb, CTL epitopes, HTL epitopes, and LBL epitopes. Through the analysis of the ProtParam server, vaccine 1 consisted of 372 amino acids S, and its molecular weight was 38707.91 g/mol. the theoretical pI of vaccine I was 7.81. Vaccine 2 contained 318 amino acids, its molecular weight was 33206.34 g/mol, and the theoretical pI was 9.41. These results describe the basic properties of vaccine constructors. Vaccine 1's instability index was 13.09, while that of vaccine 2 was 21.69, which suggests that both vaccines are stable. The aliphatic indices of vaccine 1 and vaccine 2 were 53.82 and 58.33, respectively, which revealed that both vaccines were thermostable. The GRAVY (GR and AVerage of hydropathy) index of vaccine 1 and vaccine 2 were -0.692 and -0.612, respectively, which demonstrated the vaccines' hydrophilic nature. Both vaccines' half-life in vitro of mammalian reticulocytes cytes is 30 hours while in vivo of *yeast* is more than 20 hours and 10 hours in vivo of *E. coli*. The antigenicity of vaccine 1 was 1.0738 and 0.946426, respectively, as predicted by Vaxijen2.0 and AITIGENpro. The antigenicity of vaccine 2 predicted by Vaxijen2.0 and ANTIGENpro was 0.9932 and 0.942819, respectively. The SQLpro predicts that the dissolution probability of vaccine 1 and vaccine 2 is 0.906464 and 0.892241, respectively, when overexpressed in *E. coli*. Furthermore, the AllerTOP 2.0 and Algpred servers predicted that neither vaccine was allergic.

Secondary structure prediction

The Prabi server reported secondary structure prediction, in which vaccine 1 contained 21.51% alpha-helices, 18.01% extended strands, and 60.48% random coils. For vaccine 2, the secondary structure included 21.38% alpha-helices, 19.18% extended strands, and 59.43% random coils.

Modeling and validation of vaccine

First, the RaptorX server was used to predict a primary 3D structure for the vaccine sequence. Coarse models were updated to the Galaxy server for refinement. GDT-HA, MolProbity, and RMSD plots were used to assess the models. The best models are exhibited in the figures. Vaccine 1 gets an ERRAT score of 80.000. The ERRAT score of the vaccine2 is 90.400. The Ramachandran plot analysis revealed that 83.2% of residues lied in the most favorable areas, and 14.0% of residues lied in additional permitted areas. Moreover, the Ramachandran plot of vaccine 1 showed that. For vaccine 2, 81.5% of residues were in the most favorable areas, and 16.0% of residues were in gerenally permitted areas. The Z scores of vaccines 1 and 2 were -4.93 and -4.62, respectively. Figure 2 **here**, Figure 3 **here.**

Immune Simulations

Immune stimulation was programmed using the C-IMMSIM server. The results of the host immune system's response to the designed vaccines 1 and 2 are shown in Figure 3. The primary, secondary and final immune responses have an important contribution to vaccine immunity. In particular, high antibody titers were observed, first with high titers IgG and IgM, followed by IgG1 and IgG2. The antibody titer induced by vaccine 1 was higher than that induced by vaccine 2. Furthermore, in the results of two vaccine simulations, B cells were stimulated and proliferated, which resulted in memory cell development. Meanwhile, the upregulation of the population of cytotoxic and helper T cells indicates that the immune response develops after vaccine injection. At the same time, high IFN-γ, IL-2, and IL-10 levels were induced by the designed vaccine. These results indicated that the host produced an effective immune response to the vaccine through immune stimulation. The immune cell population stimulated can be found in Figure S2. Figure 4 **here**.

Molecular docking

To assess the binding ability of the designed vaccine and antigenic receptors, we used HADDOCK server 2.4 to stimulate docking progress. The A chains of TLR2 and TLR4 were used for molecular docking. In the results of TLR2 and vaccine 1 docking, the best HADDOCK score of the cluster was -148.5 +/- 1.4. Similarly, the results of TLR2 and vaccine 2 docking revealed that the HADDOCK score of the cluster was -146.5 +/- 1.9. In the condition of vaccine 1 and TLR4 docking, the highest score of the structure was -222.1 +/- 3.8. For vaccine2 and TLR4, the great HADDOCK score of the cluster was -163.2 +/- 3.1.

Moreover, the α chains of MHCI and MHC II molecules were used for molecular docking with vaccine constructors. For vaccine 1 and the MHCI molecule, the best structure had a HADDOCK score of -193.9 +/- 5.3. Similarly, the vaccine2 and MHCI molecular results indicated that the best structure had a HADDOCK score of -137.4 +/- 1.6. For the vaccine1 and MHC II molecular, the best structure had a HADDOCK score of -172.2 +/- 1.5 and a while for vaccine2 and MHC II molecular, the best structure had a HADDOCK score of -184.2 +/- 1.6 and a. BCR is also tested for docking with vaccines, for vaccine 1 and BCR, the best structure had a HADDOCK score of -217.3 +/- 1.4 and a z score of -2.2. The results of vaccine 2 and BCR molecules indicated that the best structure had a HADDOCK score of -149.6 +/- 3.6.

The models with better scores were selected, and these complexes were further refined by HADDOCK. Then, the server generated 20 refined models into one cluster, which symbolized 100% water-refined models. The data of the interactions between the designed vaccines and receptors from their refined structures are shown in the figure, and complexes are shown in Table S4 and S5.

Docking analysis

Then, the vaccine-receptor complexes were submitted to PDBsum to analyze the interaction interface. In the results, 4 salt bridges and 15 hydrogen bonds were revealed between vaccine 1 and TLR2, while the same data for vaccine 2 were 4 and 15. For TLR4, vaccine 1 seemed to establish 3 salt bridges and 23 hydrogen bonds, while vaccine 2 formed 4 and 13. The number of salt bridges and hydrogen bonds built between vaccine 1 and HLAA1101 was 6 and 16 hydrogen bonds, which were 3 and 14 for vaccine 2, respectively. Two salt bridges and 11 hydrogen bonds seemed to be built between vaccine 1 and HLADRB0401, while vaccine 2 formed 4 and 10 bonds. Finally, between BCR and vaccine 1, there were 3 salt bridges and 16 hydrogen bonds, while between BCR and vaccine 2, there were 4 and 13.

We further analyzed interaction residues between vaccine 1 and TLR2, which were 33 and 30, covering 1327 Å² and 1356 Å², respectively. Similarly, the interaction residues between vaccine 1 and TLR4 were 27 and 28, covering 1593 Å² and 1629 Å², the interaction residues between vaccine 1 and HLA1101 were 30 and 25, covering 1656 Å² and 1579 Å², and the interaction residues between vaccine 1 and HLADRB0401 were 28 and 26, covering 1458 Å² and 1519 Å², respectively. The interaction residues between vaccine1 and BCR were 27 and 35, covering 1790 Å² and 1630 Å², respectively.

In addition, the interaction residues for vaccine 2 and TLR2 were 33 and 30, covering 1327 Å² and 1356 Å², respectively. Similarly, vaccine 2 and TLR4 each had 19 and 24 residues to interact with, covering 1106 Å² and 1006 Å² areas, respectively. Finally, the interacting residues between vaccine 2 and HLA-1101 were 16 and 21, covering 1276 Å² and 1166 Å², and the interacting residues between vaccine 2 and MHCII were 24 and 27, covering 1419 Å² and 1372 Å², respectively. while the interaction residues between

vaccine2 and BCR were 20 and 21, covering 1226 Å² and 1162 Å². The docked complex between vaccines and HLA-1101 and TLR2 is exhibited below in Figure 5, and the remaining receptors and vaccine complex can be found in Figure S3. Figure 5 **here**

Population Coverage Analysis

MHC allele distribution varies with geographic region and ethnicity. Therefore, population coverage analysis needs to be considered when an effective vaccine is designed. The screened CTL and HTL epitopes were predicted for their coverage in the global population; the global population coverage for Vaccine 1 was 84.38%, while that of Vaccine 2 was 92.28%. The results of population coverage analysis could be found in Figure S4.

Molecular Dynamic simulation

To test the stability of vaccine-receptor complexes by molecular dynamics simulation, the iMods server was chosen. This server showed the collective motion of biological macromolecules through normal mode analysis (NMA) in internal (dihedral) coordinates. The vaccine1-HLA-A11:01 complex had an elgenvalue of 2.334594e-5 (figure 6b). The deformability of the omposite was determined by the deformation of a single residue, and the result of the vaccine1-HLA-A11:01 complex is shown in Figure 6b. The value of factor B was proportional to RMS normal mode analysis (figure 6a). The covariance matrix represented the coupling between residue pairs, and different colors indicated that different residue pairs experienced correlated (red), uncorrelated (white) or anti-correlated (blue) movements (figure 6d). The elastic network model showed which atoms were connected by springs, as shown in figure 6e. Each dot represents a spring, and the stiffness of the spring is proportional to the color depth of the dot. The gray area in the figure indicates that the connection between atoms was relativelystable. Other results are shown in Supplementary materials Figure S5. Figure 6 **here**

In silico cloning

To fuse the vaccine with the vector and ensure maximal protein expression in *E. coli (strain K12)*, we used the Java Codon Adaptation Tool (JCat) to optimize the concentration of vaccine protein. Codon-optimized sequence 1 was 1000 nucleotides with a CAI value of 0.990 and a GC content of 0.51. Codon-optimized sequence 2 had 1065 nucleotides, with a 0.988 CAI value and a GC content of 0.51. Two groups of data indicated that the proteins could be expressed well in *E. coli*. Then, the *Bam*HI and *Xho*I restriction sites were added to the codon sequence, *Bam*HI to the 5' end and *Eco*RI to the 3' end. Finally, the whole sequence inside the Pet-28a (+) plasmid was cloned to ensure the designed expression in *E. coli*. The nucleotide sequences of vaccines are shown in figure S6. Figure 7 **here**

Discussion

Acinetobacter baumannii is a Gram-negative, obligate aerobe coccobacillus. During the past decade, research has greatly improved our understanding of *A. baumannii*, and its pathogenesis has been described in detail(Morris et al.). Its characteristic multidrug resistance has already broken our last antibiotic defense comprises carbapenems, colistin, and tigecycline to some extent(Asif et al.). To accelerate the progression of vaccine development, some researchers have already started to use immunoinformatic methods. Touhidinia et al designed an MEV based on the CarO protein, which is connected to carbapenem resistance(Touhidinia et al.). Ahmad et al developed another MEV based on the proteins BamA, FimD, and Rhs aiming to combat tigecycline resistance(Ahmad et al.). Other attempts were based on epitope analysis of the gacS protein(Smiline Girija) or reverse vaccinology(Shahid et al.). In the process of in silco vaccine design, target selection is important. The studies above were focused on different proteins, but each protein's role in *baumannii* pathogenesis is well studied. While our objective is to design an MEV based on OmpA, OmpW, and Omp33-36, in addition to solid evidence that injecting outer membrane complexes causes a protective immune response(McConnell et al.), an in silco designed epitope peptide from OmpA causing an immune response in mice is also considered(Mehdinejadiani et al.).

A recent study shows that microevolution of the OmpA protein may lead to reduced efficacy of drugs or vaccines developed with OmpA as the target(Viale and Evans). To avoid this potential problem, OmpW and Omp33-36 were chosen for the advancement of the vaccine. OmpW is involved in iron uptake by *Acinetobacter baumannii*, which is conserved in 804 *Acinetobacter baumannii* strains with > 91% identity(Huang et al.). Conservation for Omp33-36 is as high as 98% among more than 1600 strains of *Acinetobacter baumannii*(Huang et al.). Meanwhile, designing a vaccine based on a single protein may only provide some protection against infection(McConnell and Martin-Galiano). In this method, we designed two vaccines based on OmpA, OmpW, and Omp33-36.

Outer membrane proteins (OMPs) are a series of β-barrel structured proteins anchored in the outer membrane. Some OMPs are chosen as potential vaccine targets. Outer membrane protein A (OmpA), outer membrane W (OmpW), and 33-36 kDa Omp (Omp33-36) are all porins on the outer membrane and responsible for the pathogenicity of *A. baumannii*. These proteins are firmly connected with the virulence and antibiotic resistance of *A. baumannii* by participating in adherence, invasion, induction of apoptosis, serum resistance, biofilm formation and persistence(Lee et al. 2017; Smani et al. 2013; Uppalapati et al. 2020). Outer membrane protein A (OmpA) is one of the most abundant OMPs and has incredible potential as a therapeutic target(Nie et al. 2020). Recombinant OmpA (rOmpA) with aluminum hydroxide as an adjuvant can improve survival in infected mice(Luo et al. 2012), mucosal immunization with rOmpA can reduce death from *A. baumannii* infection(Zhang et al. 2016), while a DNA vaccine encoding OmpA showed pronounced defensive adequacy in a pneumonia mouse model(Lei et al. 2019). However, as the most discussed Omp, a high-recurrence microevolution could limit the efficiency of vaccines dependent only on OmpA(Viale and Evans 2020). In the meantime, mice immunized with OmpW responded with an increase in specific IgG and survival(Huang et al. 2015) and other research showed Omp33-36 as potential targets to cause protective immunity(Novovic et al. 2018) and both proteins are considered to be converse. Subsequently, OmpW and Omp33 are applied to frame vaccines along with OmpA to ensure the validity of the final MEV.

Another important part of the vaccine is adjuvants. In this case, we selected type II heat-labile (LT-II) enterotoxins from *Escherichia coli* to form vaccines, and their sequences LT-IIc and LT-IIb can enhance $CD8^+$ T cell immunity when combined with antigens(Hu et al. 2014), which is conferred upon their ganglioside-binding B subunits(Hu et al. 2015).

Epitope prediction and selection make up the framework of in silco vaccine design. In the selection of epitopes, especially for CTL and HTL epitopes, we compared outcomes from different servers and enlarged the range of MHC alleles to choose those overlapping results as much as possible. For further filtering of epitopes, epitopes are tested for their ability to induce cytokines. As a result, two vaccines were developed: Vaccine 1 contains 5 CTL epitopes, 2 are from OmpA, and 3 are from Omp33, 4 HLT epitopes, half of which are from OmpA while the else are from Omp33, 7 LBL epitopes, 4 are from OmpA and 3 are from Omp33. Vaccine 2 was developed based on OmpA and OmpW and consists of 4 CTL epitopes: 1 is from OmpA and 3 are from OmpW, 4 HTL epitopes, 2 epitopes are formed OmpA and 2 is from OmpW, and 5 LBL epitopes, 3 are from OmpA and 2 are from OmpW. In the selection of predicted epitopes, antigenicity is emphasized considering that antigenicity refers to the ability to resist antibodies or sensitive lymphocytes specifically induced, the antigenicity of the two vaccines is similar, and both are nontoxic, nonallergic, and highly immunogenic. The vaccine constructors were then docked with TLR2, TLR4, and MHCI molecules to show that the vaccine can induce host immunity. HADDOCK was used for the docking server. As an experimental knowledge-driven server, HADDOCK performed well in the Capri blind docking test(de Vries et al.) and is used widely in medicine and vaccine design. Docking results were mainly evaluated by RMSD plots and docking surface analyses, strong bindings between vaccine and receptors are shown by docking surface analyses and RMSD plots revealed the stability of the vaccine-receptor complex structure, by analyzing the docking interface of the vaccine receptor complex, the larger docking area of vaccine 1-receptor indicates that vaccine 1 has a better immune induction effect on the host. Through immune stimulation, the effectiveness of the vaccine has been proven in theory, while vaccine 1 can induce higher antibody titers than the vaccine. The world population coverage rate of Vaccine 2 is higher than that of Vaccine 1. In the end, these two vaccines are effective vaccines through informatics simulation calculations, and the results of immune simulation indicate that both vaccines can induce protective reactions in theory.

Compared with the traditional method of vaccine development, designing vaccines by immunoinformatics costs less, and the screening of epitopes and the design of vaccines are faster. Multiepitope vaccines have lower toxicity, lower allergies and higher safety than traditional vaccines. The multiepitope vaccine we designed contains CTL epitopes, HTL epitopes, and LBL epitopes, which can trigger both humoral and cellular immunity in the host. At the same time, the combination of epitopes of two different proteins can fight *Acinetobacter baumannii* infection more effectively. However, it may take some time to further verify the performance of the vaccine against *Acinetobacter baumannii* in vivo and in vitro.

Abbreviations

Cytotoxic T-lymphocyte (CTL); Grand average of hydropathicity (GRAVY); Helper T-lymphocyte (HTL); Linear B cell (LBL); Major histocompatibility complex (MHC); Multidrug-resistant (MDR); Outer membrane protein A (OmpA); Outer membrane protein33-36 (Omp33-36); Outer membrane W (OmpW); Position-specific scoring matrix (PSSM); Toll-like receptors (TLRs); Type II heat-labile (LT-II); Ventilator-associated pneumonia (VAP).

Declarations

Ethics approval and consent to participate:

Not applicable (This study does not report on or involve any animals, humans, human data, human tissue or plants).

Consent for publication:

Not applicable (This study does not contain any individual person's data).

Availability of data and materials:

The datasets generated and analyzed for this study are available from the corresponding author upon reasonable request.

Competing interests:

The authors declare that they have no competing interests.

Funding:

1. The National Natural Science Foundation of China (No. 81770080)

2. Supported by the Project Program of National Clinical Research Center for Geriatric Disorders (Xiang ya Hospital, Grant No. 2020LNJJ05)

3. The National Natural Science Foundation of China (No. 8210012334)

4. National Key R&D Program of China (No. 2016YFC1304204)

Author Contributions:

Conceptualization, F. Z and S.M.; methodology, F.Z.; validation, S.M. and M.R.; formal analysis, P. Z, W. P, H. Y and Y. C; writing—original draft preparation, S. M and C. T; writing—review and editing: J. C; supervision, P. P and J.C.; project administration, P. P and J. C; funding acquisition, P. P

Acknowledgements

Thanks to the support of M. Cheung

References

1. Ahmad S, Ranaghan KE, Azam SS (2019) Combating tigecycline resistant *Acinetobacter baumannii*: A leap forward towards multi-epitope based vaccine discovery. Eur J Pharm Sci 132:1-17 doi:10.1016/j.ejps.2019.02.023
2. Amanna IJ, Slifka MK (2011) Contributions of humoral and cellular immunity to vaccine-induced protection in humans. Virology 411(2):206-15 doi:10.1016/j.virol.2010.12.016
3. Asif M, Alvi IA, Rehman SU (2018) Insight into *Acinetobacter baumannii*: pathogenesis, global resistance, mechanisms of resistance, treatment options, and alternative modalities. Infect Drug Resist 11:1249-1260 doi:10.2147/IDR.S166750
4. Bui HH, Sidney J, Dinh K, Southwood S, Newman MJ, Sette A (2006) Predicting population coverage of T-cell epitope-based diagnostics and vaccines. BMC Bioinformatics 7:153 doi:10.1186/1471-2105-7-153

5. Calis JJ, Maybeno M, Greenbaum JA, Weiskopf D, De Silva AD, Sette A, Kesmir C, Peters B (2013) Properties of MHC class I presented peptides that enhance immunogenicity. PLoS Comput Biol 9(10):e1003266 doi:10.1371/journal.pcbi.1003266
6. De Oliveira DMP, Forde BM, Kidd TJ, Harris PNA, Schembri MA, Beatson SA, Paterson DL, Walker MJ (2020) Antimicrobial Resistance in *ESKAPE* Pathogens. Clin Microbiol Rev 33(3) doi:10.1128/CMR.00181-19
7. de Vries SJ, van Dijk M, Bonvin AM (2010) The HADDOCK web server for data-driven biomolecular docking. Nat Protoc 5(5):883-97 doi:10.1038/nprot.2010.32
8. Dhanda SK, Gupta S, Vir P, Raghava GP (2013a) Prediction of IL4 inducing peptides. Clin Dev Immunol 2013:263952 doi:10.1155/2013/263952
9. Dhanda SK, Vir P, Raghava GP (2013b) Designing of interferon-gamma inducing MHC class-II binders. Biol Direct 8:30 doi:10.1186/1745-6150-8-30
10. Doytchinova IA, Flower DR (2007) Identifying candidate subunit vaccines using an alignment-independent method based on principal amino acid properties. Vaccine 25(5):856-66 doi:10.1016/j.vaccine.2006.09.032
11. Foroutan M, Ghaffarifar F, Sharifi Z, Dalimi A (2020) Vaccination with a novel multi-epitope ROP8 DNA vaccine against acute *Toxoplasma gondii* infection induces strong B and T cell responses in mice. Comp Immunol Microbiol Infect Dis 69:101413 doi:10.1016/j.cimid.2020.101413
12. Garnier J, Gibrat JF, Robson B (1996) GOR method for predicting protein secondary structure from amino acid sequence. Methods Enzymol 266:540-53 doi:10.1016/s0076-6879(96)66034-0
13. Gellings PS, Wilkins AA, Morici LA (2020) Recent Advances in the Pursuit of an Effective *Acinetobacter baumannii* Vaccine. Pathogens 9(12) doi:10.3390/pathogens9121066
14. Grandi A, Fantappie L, Irene C, Valensin S, Tomasi M, Stupia S, Corbellari R, Caproni E, Zanella I, Isaac SJ, Ganfini L, Frattini L, Konig E, Gagliardi A, Tavarini S, Sammicheli C, Parri M, Grandi G (2018) Vaccination With a FAT1-Derived B Cell Epitope Combined With Tumor-Specific B and T Cell Epitopes Elicits Additive Protection in Cancer Mouse Models. Front Oncol 8:481 doi:10.3389/fonc.2018.00481
15. Grote A, Hiller K, Scheer M, Munch R, Nortemann B, Hempel DC, Jahn D (2005) JCat: a novel tool to adapt codon usage of a target gene to its potential expression host. Nucleic Acids Res 33(Web Server issue):W526-31 doi:10.1093/nar/gki376
16. Gu Y, Sun X, Li B, Huang J, Zhan B, Zhu X (2017) Vaccination with a Paramyosin-Based Multi-Epitope Vaccine Elicits Significant Protective Immunity against *Trichinella spiralis* Infection in Mice. Front Microbiol 8:1475 doi:10.3389/fmicb.2017.01475
17. Gupta S, Kapoor P, Chaudhary K, Gautam A, Kumar R, Open Source Drug Discovery C, Raghava GP (2013) In silico approach for predicting toxicity of peptides and proteins. PLoS One 8(9):e73957 doi:10.1371/journal.pone.0073957
18. Guruprasad K, Reddy BV, Pandit MW (1990) Correlation between stability of a protein and its dipeptide composition: a novel approach for predicting in vivo stability of a protein from its primary sequence. Protein Eng 4(2):155-61 doi:10.1093/protein/4.2.155
19. He Y, Rappuoli R, De Groot AS, Chen RT (2010) Emerging vaccine informatics. J Biomed Biotechnol 2010:218590 doi:10.1155/2010/218590
20. Honorato RV, Koukos PI, Jimenez-Garcia B, Tsaregorodtsev A, Verlato M, Giachetti A, Rosato A, Bonvin A (2021) Structural Biology in the Clouds: The WeNMR-EOSC Ecosystem. Front Mol Biosci 8:729513 doi:10.3389/fmolb.2021.729513
21. Hu JC, Greene CJ, King-Lyons ND, Connell TD (2015) The Divergent CD8+ T Cell Adjuvant Properties of LT-IIb and LT-IIc, Two Type II Heat-Labile Enterotoxins, Are Conferred by Their Ganglioside-Binding B Subunits. PLoS One 10(11):e0142942 doi:10.1371/journal.pone.0142942
22. Hu JC, Mathias-Santos C, Greene CJ, King-Lyons ND, Rodrigues JF, Hajishengallis G, Ferreira LC, Connell TD (2014) Intradermal administration of the Type II heat-labile enterotoxins LT-IIb and LT-IIc of enterotoxigenic *Escherichia coli* enhances humoral and CD8+ T cell immunity to a co-administered antigen. PLoS One 9(12):e113978 doi:10.1371/journal.pone.0113978
23. Huang W, Wang S, Yao Y, Xia Y, Yang X, Long Q, Sun W, Liu C, Li Y, Ma Y (2015) OmpW is a potential target for eliciting protective immunity against *Acinetobacter baumannii* infections. Vaccine 33(36):4479-85 doi:10.1016/j.vaccine.2015.07.031
24. Huang W, Yao Y, Wang S, Xia Y, Yang X, Long Q, Sun W, Liu C, Li Y, Chu X, Bai H, Yao Y, Ma Y (2016) Immunization with a 22-kDa outer membrane protein elicits protective immunity to multidrug-resistant *Acinetobacter baumannii*. Sci Rep 6:20724 doi:10.1038/srep20724

25. Ivashkiv LB (2018) IFNgamma: signalling, epigenetics and roles in immunity, metabolism, disease and cancer immunotherapy. Nat Rev Immunol 18(9):545-558 doi:10.1038/s41577-018-0029-z
26. Ko J, Park H, Heo L, Seok C (2012) GalaxyWEB server for protein structure prediction and refinement. Nucleic Acids Res 40(Web Server issue):W294-7 doi:10.1093/nar/gks493
27. Kyriakidis I, Vasileiou E, Pana ZD, Tragiannidis A (2021) *Acinetobacter baumannii* Antibiotic Resistance Mechanisms. Pathogens 10(3) doi:10.3390/pathogens10030373
28. Larsen MV, Lundegaard C, Lamberth K, Buus S, Lund O, Nielsen M (2007) Large-scale validation of methods for cytotoxic T-lymphocyte epitope prediction. BMC Bioinformatics 8:424 doi:10.1186/1471-2105-8-424
29. Laskowski RA, Jablonska J, Pravda L, Varekova RS, Thornton JM (2018) PDBsum: Structural summaries of PDB entries. Protein Sci 27(1):129-134 doi:10.1002/pro.3289
30. Lee CR, Lee JH, Park M, Park KS, Bae IK, Kim YB, Cha CJ, Jeong BC, Lee SH (2017) Biology of *Acinetobacter baumannii*: Pathogenesis, Antibiotic Resistance Mechanisms, and Prospective Treatment Options. Front Cell Infect Microbiol 7:55 doi:10.3389/fcimb.2017.00055
31. Lei L, Yang F, Zou J, Jing H, Zhang J, Xu W, Zou Q, Zhang J, Wang X (2019) DNA vaccine encoding OmpA and Pal from *Acinetobacter baumannii* efficiently protects mice against pulmonary infection. Mol Biol Rep 46(5):5397-5408 doi:10.1007/s11033-019-04994-2
32. Lob SH, Hoban DJ, Sahm DF, Badal RE (2016) Regional differences and trends in antimicrobial susceptibility of *Acinetobacter baumannii*. Int J Antimicrob Agents 47(4):317-23 doi:10.1016/j.ijantimicag.2016.01.015
33. Lopez-Blanco JR, Aliaga JI, Quintana-Orti ES, Chacon P (2014) iMODS: internal coordinates normal mode analysis server. Nucleic Acids Res 42(Web Server issue):W271-6 doi:10.1093/nar/gku339
34. Lotsch F, Albiger B, Monnet DL, Struelens MJ, Seifert H, Kohlenberg A, European Antimicrobial Resistance Genes Surveillance Network carbapenem-resistant *Acinetobacter baumannii* capacity survey g, group EU-Nc-rAbcs (2020) Epidemiological situation, laboratory capacity and preparedness for carbapenem-resistant *Acinetobacter baumannii* in Europe, 2019. Euro Surveill 25(45) doi:10.2807/1560-7917.ES.2020.25.45.2001735
35. Lundegaard C, Nielsen M, Lund O (2006) The validity of predicted T-cell epitopes. Trends Biotechnol 24(12):537-8 doi:10.1016/j.tibtech.2006.10.001
36. Luo G, Lin L, Ibrahim AS, Baquir B, Pantapalangkoor P, Bonomo RA, Doi Y, Adams MD, Russo TA, Spellberg B (2012) Active and passive immunization protects against lethal, extreme drug resistant-*Acinetobacter baumannii* infection. PLoS One 7(1):e29446 doi:10.1371/journal.pone.0029446
37. Ma C, McClean S (2021) Mapping Global Prevalence of *Acinetobacter baumannii* and Recent Vaccine Development to Tackle It. Vaccines (Basel) 9(6) doi:10.3390/vaccines9060570
38. Magnan CN, Randall A, Baldi P (2009) SOLpro: accurate sequence-based prediction of protein solubility. Bioinformatics 25(17):2200-7 doi:10.1093/bioinformatics/btp386
39. Magnan CN, Zeller M, Kayala MA, Vigil A, Randall A, Felgner PL, Baldi P (2010) High-throughput prediction of protein antigenicity using protein microarray data. Bioinformatics 26(23):2936-43 doi:10.1093/bioinformatics/btq551
40. March C, Regueiro V, Llobet E, Moranta D, Morey P, Garmendia J, Bengoechea JA (2010) Dissection of host cell signal transduction during *Acinetobacter baumannii*-triggered inflammatory response. PLoS One 5(4):e10033 doi:10.1371/journal.pone.0010033
41. McConnell MJ, Dominguez-Herrera J, Smani Y, Lopez-Rojas R, Docobo-Perez F, Pachon J (2011) Vaccination with outer membrane complexes elicits rapid protective immunity to multidrug-resistant *Acinetobacter baumannii*. Infect Immun 79(1):518-26 doi:10.1128/IAI.00741-10
42. McConnell MJ, Martin-Galiano AJ (2021) Designing Multi-Antigen Vaccines Against *Acinetobacter baumannii* Using Systemic Approaches. Front Immunol 12:666742 doi:10.3389/fimmu.2021.666742
43. Mehdinejadiani K, Bandehpour M, Hashemi A, Ranjbar MM, Taheri S, Jalali SA, Mosaffa N (2019) In Silico Design and Evaluation of *Acinetobacter baumannii* Outer Membrane Protein a Antigenic Peptides As Vaccine Candidate in Immunized Mice. Iran J Allergy Asthma Immunol 18(6):655-663 doi:10.18502/ijaai.v18i6.2178
44. Meng X, Fu J, Zheng Y, Qin W, Yang H, Cao D, Lu H, Zhang L, Du Z, Pang J, Li W, Guo H, Du J, Li C, Wu D, Wang H (2021) Ten-Year Changes in Bloodstream Infection With *Acinetobacter Baumannii* Complex in Intensive Care Units in Eastern China: A

Retrospective Cohort Study. Front Med (Lausanne) 8:715213 doi:10.3389/fmed.2021.715213

45. Moise L, De Groot AS (2006) Putting immunoinformatics to the test. Nat Biotechnol 24(7):791-2 doi:10.1038/nbt0706-791
46. Morris FC, Dexter C, Kostoulias X, Uddin MI, Peleg AY (2019) The Mechanisms of Disease Caused by *Acinetobacter baumannii*. Front Microbiol 10:1601 doi:10.3389/fmicb.2019.01601
47. Munoz-Price LS, Weinstein RA (2008) *Acinetobacter* infection. N Engl J Med 358(12):1271-81 doi:10.1056/NEJMra070741
48. Nasr P (2020) Genetics, epidemiology, and clinical manifestations of multidrug-resistant *Acinetobacter baumannii*. J Hosp Infect 104(1):4-11 doi:10.1016/j.jhin.2019.09.021
49. Nezafat N, Ghasemi Y, Javadi G, Khoshnoud MJ, Omidinia E (2014) A novel multi-epitope peptide vaccine against cancer: an in silico approach. J Theor Biol 349:121-34 doi:10.1016/j.jtbi.2014.01.018
50. Nie D, Hu Y, Chen Z, Li M, Hou Z, Luo X, Mao X, Xue X (2020) Outer membrane protein A (OmpA) as a potential therapeutic target for *Acinetobacter baumannii* infection. J Biomed Sci 27(1):26 doi:10.1186/s12929-020-0617-7
51. Novovic K, Mihajlovic S, Dinic M, Malesevic M, Miljkovic M, Kojic M, Jovcic B (2018) *Acinetobacter* spp. porin Omp33-36: Classification and transcriptional response to carbapenems and host cells. PLoS One 13(8):e0201608 doi:10.1371/journal.pone.0201608
52. Oli AN, Obialor WO, Ifeanyichukwu MO, Odimegwu DC, Okoyeh JN, Emechebe GO, Adejumo SA, Ibeanu GC (2020) Immunoinformatics and Vaccine Development: An Overview. Immunotargets Ther 9:13-30 doi:10.2147/ITT.S241064
53. Paul S, Sidney J, Sette A, Peters B (2016) TepiTool: A Pipeline for Computational Prediction of T Cell Epitope Candidates. Curr Protoc Immunol 114:18 19 1-18 19 24 doi:10.1002/cpim.12
54. Peleg AY, Seifert H, Paterson DL (2008) *Acinetobacter baumannii*: emergence of a successful pathogen. Clin Microbiol Rev 21(3):538-82 doi:10.1128/CMR.00058-07
55. Ramirez MS, Bonomo RA, Tolmasky ME (2020) Carbapenemases: Transforming *Acinetobacter baumannii* into a Yet More Dangerous Menace. Biomolecules 10(5) doi:10.3390/biom10050720
56. Rapin N, Lund O, Bernaschi M, Castiglione F (2010) Computational immunology meets bioinformatics: the use of prediction tools for molecular binding in the simulation of the immune system. PLoS One 5(4):e9862 doi:10.1371/journal.pone.0009862
57. Reynisson B, Barra C, Kaabinejadian S, Hildebrand WH, Peters B, Nielsen M (2020) Improved Prediction of MHC II Antigen Presentation through Integration and Motif Deconvolution of Mass Spectrometry MHC Eluted Ligand Data. J Proteome Res 19(6):2304-2315 doi:10.1021/acs.jproteome.9b00874
58. Saha S, Raghava GP (2006) Prediction of continuous B-cell epitopes in an antigen using recurrent neural network. Proteins 65(1):40-8 doi:10.1002/prot.21078
59. Shahid F, Zaheer T, Ashraf ST, Shehroz M, Anwer F, Naz A, Ali A (2021) Chimeric vaccine designs against *Acinetobacter baumannii* using pan genome and reverse vaccinology approaches. Sci Rep 11(1):13213 doi:10.1038/s41598-021-92501-8
60. Smani Y, Dominguez-Herrera J, Pachon J (2013) Association of the outer membrane protein Omp33 with fitness and virulence of *Acinetobacter baumannii*. J Infect Dis 208(10):1561-70 doi:10.1093/infdis/jit386
61. Smiline Girija AS (2020) Delineating the Immuno-Dominant Antigenic Vaccine Peptides Against gacS-Sensor Kinase in *Acinetobacter baumannii*: An in silico Investigational Approach. Front Microbiol 11:2078 doi:10.3389/fmicb.2020.02078
62. Sohail MS, Ahmed SF, Quadeer AA, McKay MR (2021) In silico T cell epitope identification for *SARS-CoV-2*: Progress and perspectives. Adv Drug Deliv Rev 171:29-47 doi:10.1016/j.addr.2021.01.007
63. Steinke JW, Borish L (2001) Th2 cytokines and asthma. Interleukin-4: its role in the pathogenesis of asthma, and targeting it for asthma treatment with interleukin-4 receptor antagonists. Respir Res 2(2):66-70 doi:10.1186/rr40
64. Takahashi H, Cease KB, Berzofsky JA (1989) Identification of proteases that process distinct epitopes on the same protein. J Immunol 142(7):2221-9
65. Touhidinia M, Sefid F, Bidakhavidi M (2021) Design of a Multi-epitope Vaccine Against *Acinetobacter baumannii* Using Immunoinformatics Approach. Int J Pept Res Ther:1-21 doi:10.1007/s10989-021-10262-4
66. Uppalapati SR, Sett A, Pathania R (2020) The Outer Membrane Proteins OmpA, CarO, and OprD of *Acinetobacter baumannii* Confer a Two-Pronged Defense in Facilitating Its Success as a Potent Human Pathogen. Front Microbiol 11:589234 doi:10.3389/fmicb.2020.589234

67. van Zundert GCP, Rodrigues J, Trellet M, Schmitz C, Kastritis PL, Karaca E, Melquiond ASJ, van Dijk M, de Vries SJ, Bonvin A (2016) The HADDOCK2.2 Web Server: User-Friendly Integrative Modeling of Biomolecular Complexes. J Mol Biol 428(4):720-725 doi:10.1016/j.jmb.2015.09.014
68. Viale AM, Evans BA (2020) Microevolution in the major outer membrane protein OmpA of *Acinetobacter baumannii*. Microb Genom 6(6) doi:10.1099/mgen.0.000381
69. Wang P, Sidney J, Kim Y, Sette A, Lund O, Nielsen M, Peters B (2010) Peptide binding predictions for HLA DR, DP and DQ molecules. BMC Bioinformatics 11:568 doi:10.1186/1471-2105-11-568
70. Wang S, Sun S, Li Z, Zhang R, Xu J (2017) Accurate De Novo Prediction of Protein Contact Map by Ultra-Deep Learning Model. PLoS Comput Biol 13(1):e1005324 doi:10.1371/journal.pcbi.1005324
71. Wiederstein M, Sippl MJ (2007) ProSA-web: interactive web service for the recognition of errors in three-dimensional structures of proteins. Nucleic Acids Res 35(Web Server issue):W407-10 doi:10.1093/nar/gkm290
72. Wilkins MR, Gasteiger E, Bairoch A, Sanchez JC, Williams KL, Appel RD, Hochstrasser DF (1999) Protein identification and analysis tools in the ExPASy server. Methods Mol Biol 112:531-52 doi:10.1385/1-59259-584-7:531
73. Wold. S, Jonsson. J, Sjiistriim. M, Sandberg. M, RSinnar S (1993) DNA and peptide sequences and chemical processes multivariately modelled by principal component analysis and partial least-squares projections to latent structures. Analytica Chimica Acta doi:10.1016/0003-2670(93)80437-p
74. Xu J (2019) Distance-based protein folding powered by deep learning. Proc Natl Acad Sci U S A 116(34):16856-16865 doi:10.1073/pnas.1821309116
75. Xu J, McPartlon M, Li J (2021) Improved protein structure prediction by deep learning irrespective of co-evolution information. Nat Mach Intell 3:601-609 doi:10.1038/s42256-021-00348-5
76. Xue LC, Rodrigues JP, Kastritis PL, Bonvin AM, Vangone A (2016) PRODIGY: a web server for predicting the binding affinity of protein-protein complexes. Bioinformatics 32(23):3676-3678 doi:10.1093/bioinformatics/btw514
77. Yousafi Q, Amin H, Bibi S, Rafi R, Khan MS, Ali H, Masroor A (2021) Subtractive Proteomics and Immuno-informatics Approaches for Multi-peptide Vaccine Prediction Against *Klebsiella oxytoca* and Validation Through In Silico Expression. Int J Pept Res Ther:1-17 doi:10.1007/s10989-021-10283-z
78. Zhang X, Yang T, Cao J, Sun J, Dai W, Zhang L (2016) Mucosal immunization with purified OmpA elicited protective immunity against infections caused by multidrug-resistant *Acinetobacter baumannii*. Microb Pathog 96:20-5 doi:10.1016/j.micpath.2016.04.019
79. Zhao Z, Sun HQ, Wei SS, Li B, Feng Q, Zhu J, Zeng H, Zou QM, Wu C (2015) Multiple B-cell epitope vaccine induces a *Staphylococcus* enterotoxin B-specific IgG1 protective response against MRSA infection. Sci Rep 5:12371 doi:10.1038/srep12371

Figures

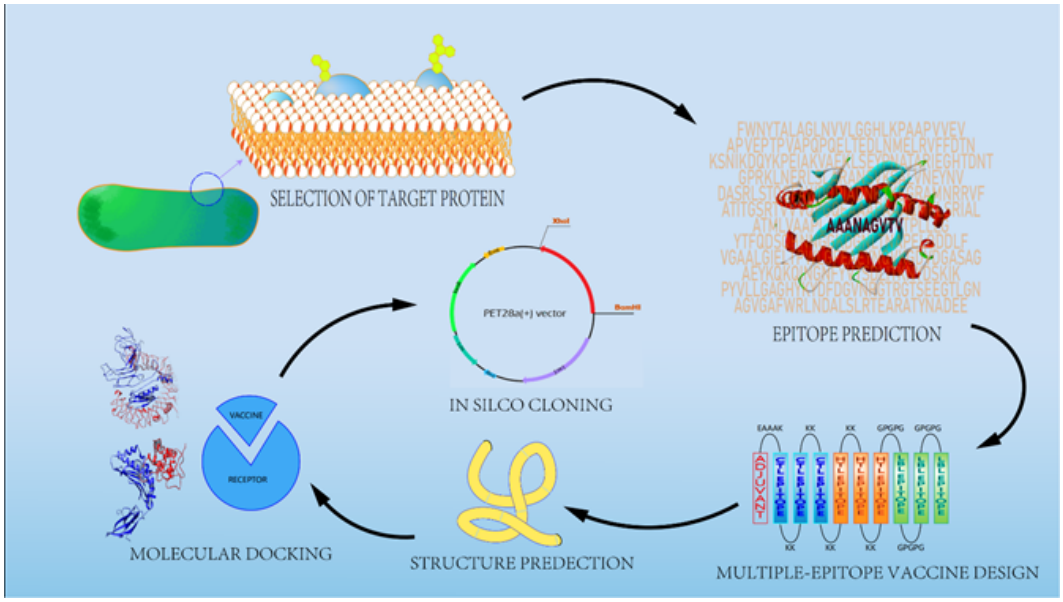

Figure 1

Process of multiepitope design and in-silco cloning

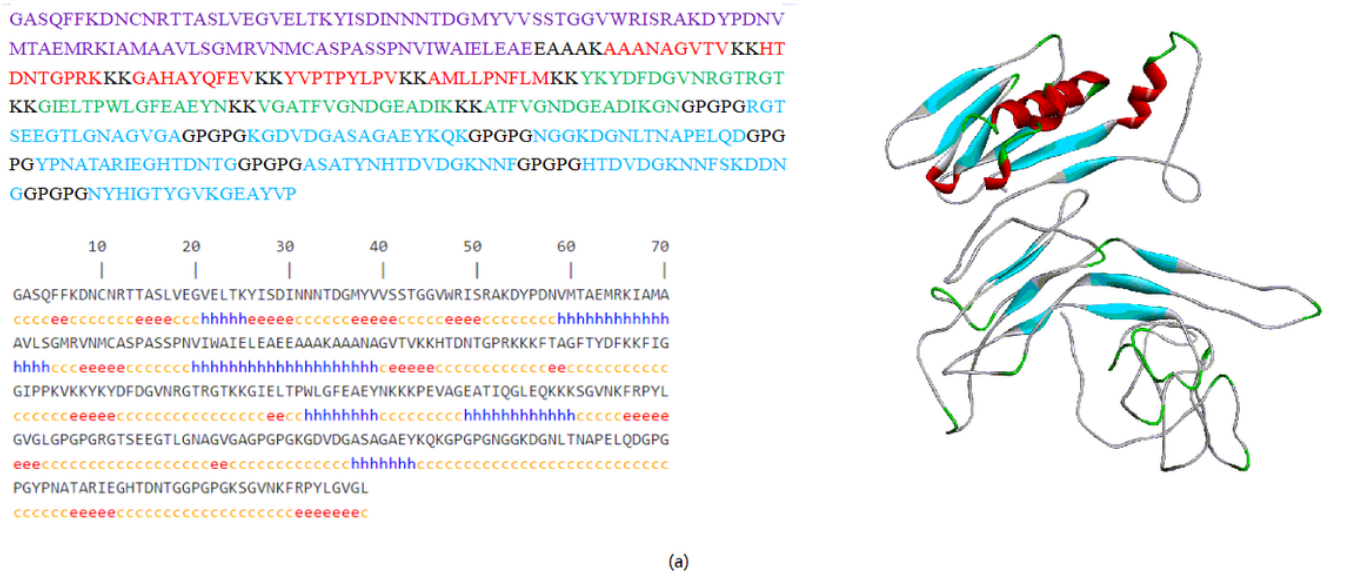

(b)

Figure 2

First, second and third structure of vaccine 1 and vaccine 2, in the first structure, purple residues stand for adjuvant sequence, red residues stand for CTL epitopes, green residues stand for HTL epitopes and blue residues stand for LBL epitopes; In the second structure, h stand for α-helix, e stand for extended strand and c stand for random coil. (a) Predicted structure of vaccine 1, (b) predicted structure of vaccine 2.

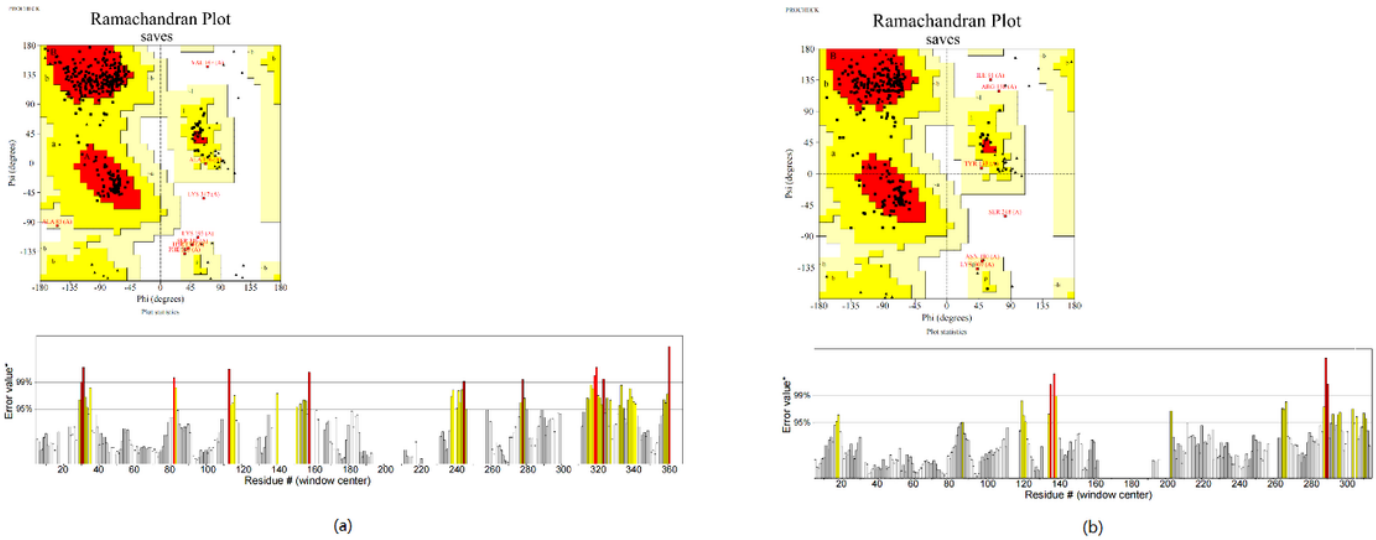

Figure 3

Ramchandran and ERRAT plot for predicted vaccine construct quality assessment, (a) Ramchandran and ERRAT plot of vaccine 1 (b) Ramchandran and ERRAT plot of vaccine 2

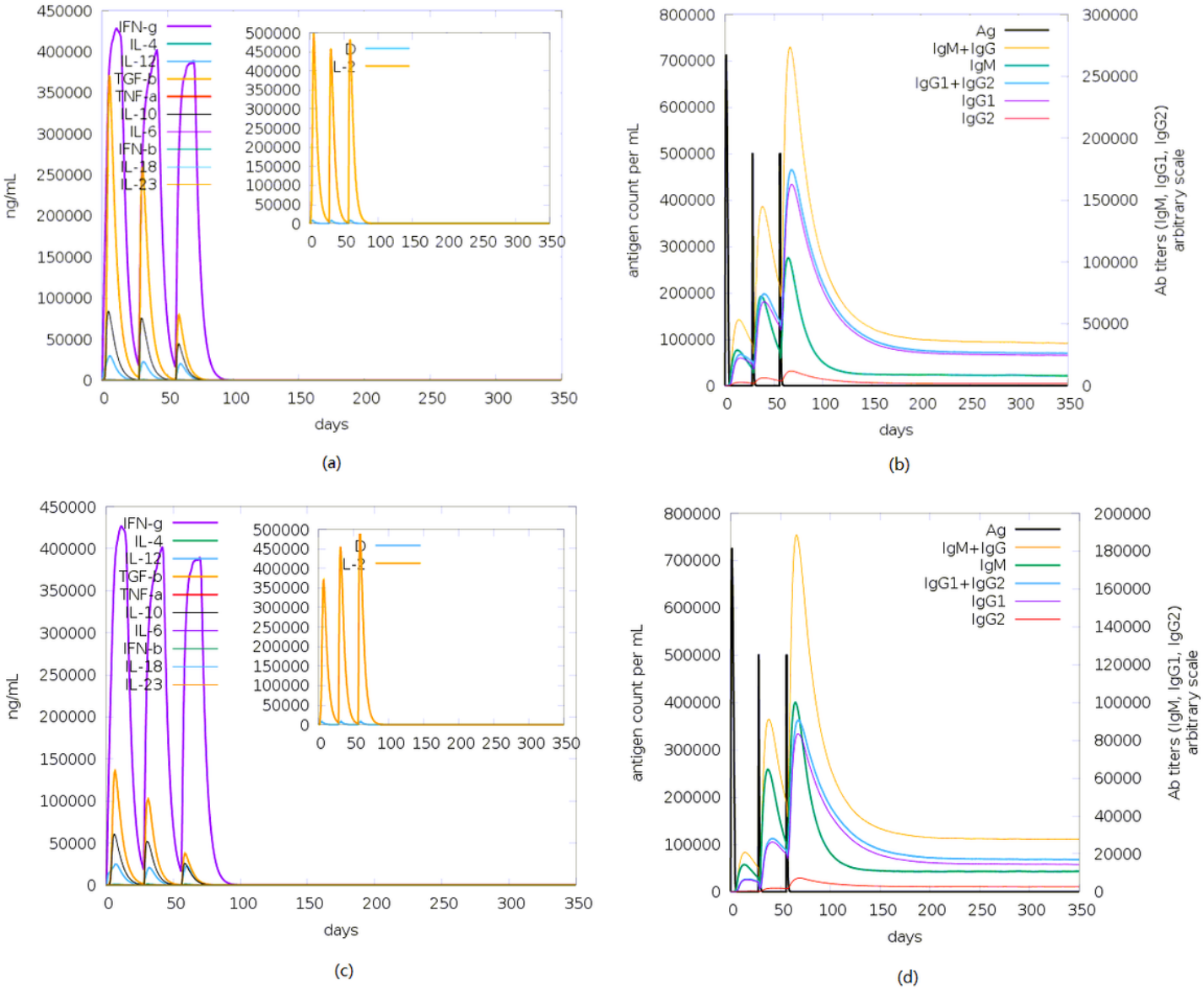

Figure 4

Immune simulation results from C-ImmSim. (a), (c) Predicted cytokine released by vaccine 1 and vaccine 2. After each injection, there was a significant increase in IFN-g and TGF-b. (b), (d) Immunoglobulin production represents proliferation of the immune response after vaccine infection. Various subtypes of immunoglobulin are represented as colored peaks, and finally, there will be a protective stable IgM and IgG concentration.

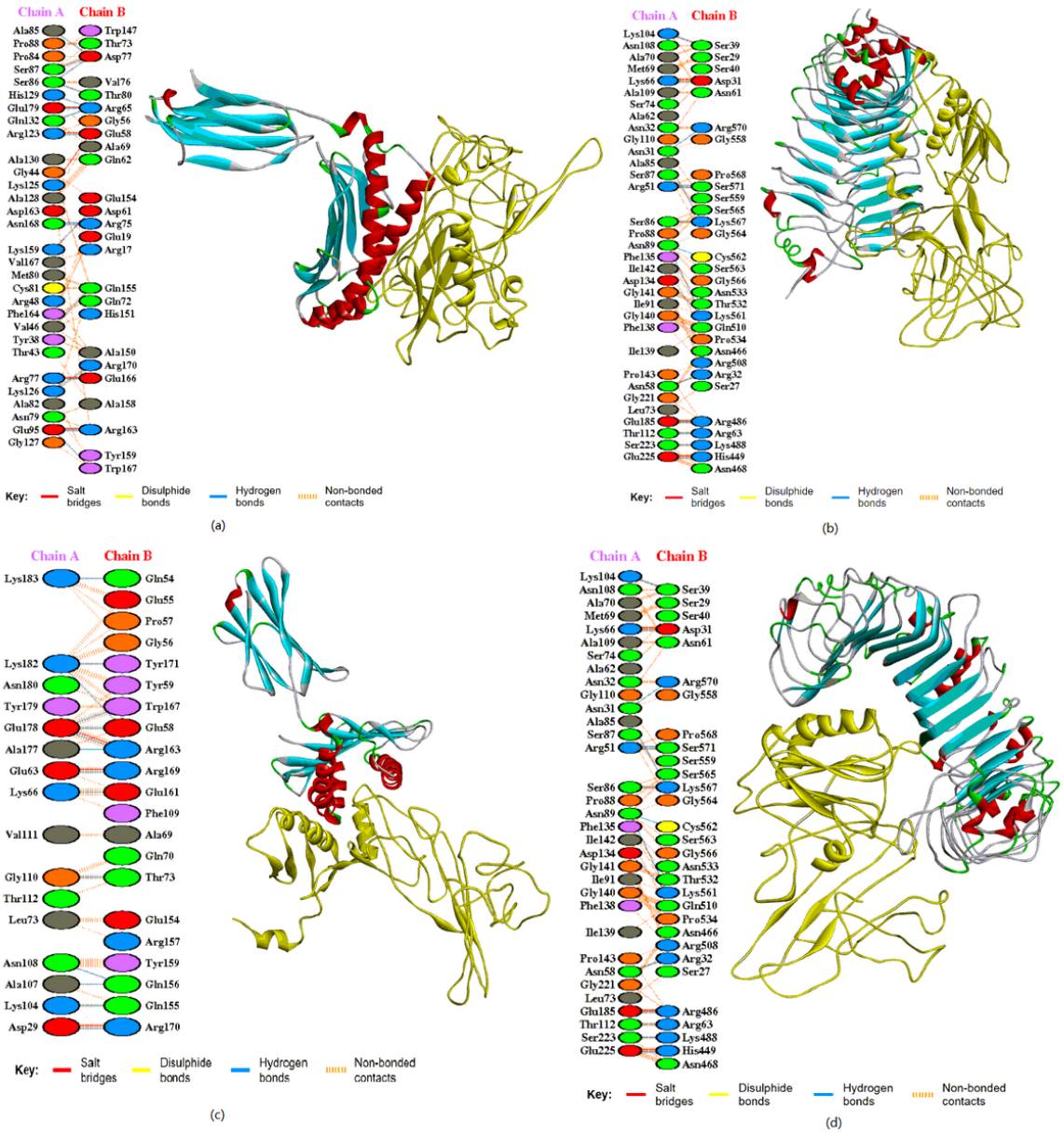

Figure 5

Docking results and interacting residues of the complex. Docked complex of vaccine construct and receptor and the interacting part along with the interacting residue, in the figure, vaccine construct is highlighted (a)Vaccine 1 and HLAA1101 (b) Vaccine 1 and TLR 2 (c) Vaccine 2 and HLAA1101 (d) Vaccine 2 and TLR 2

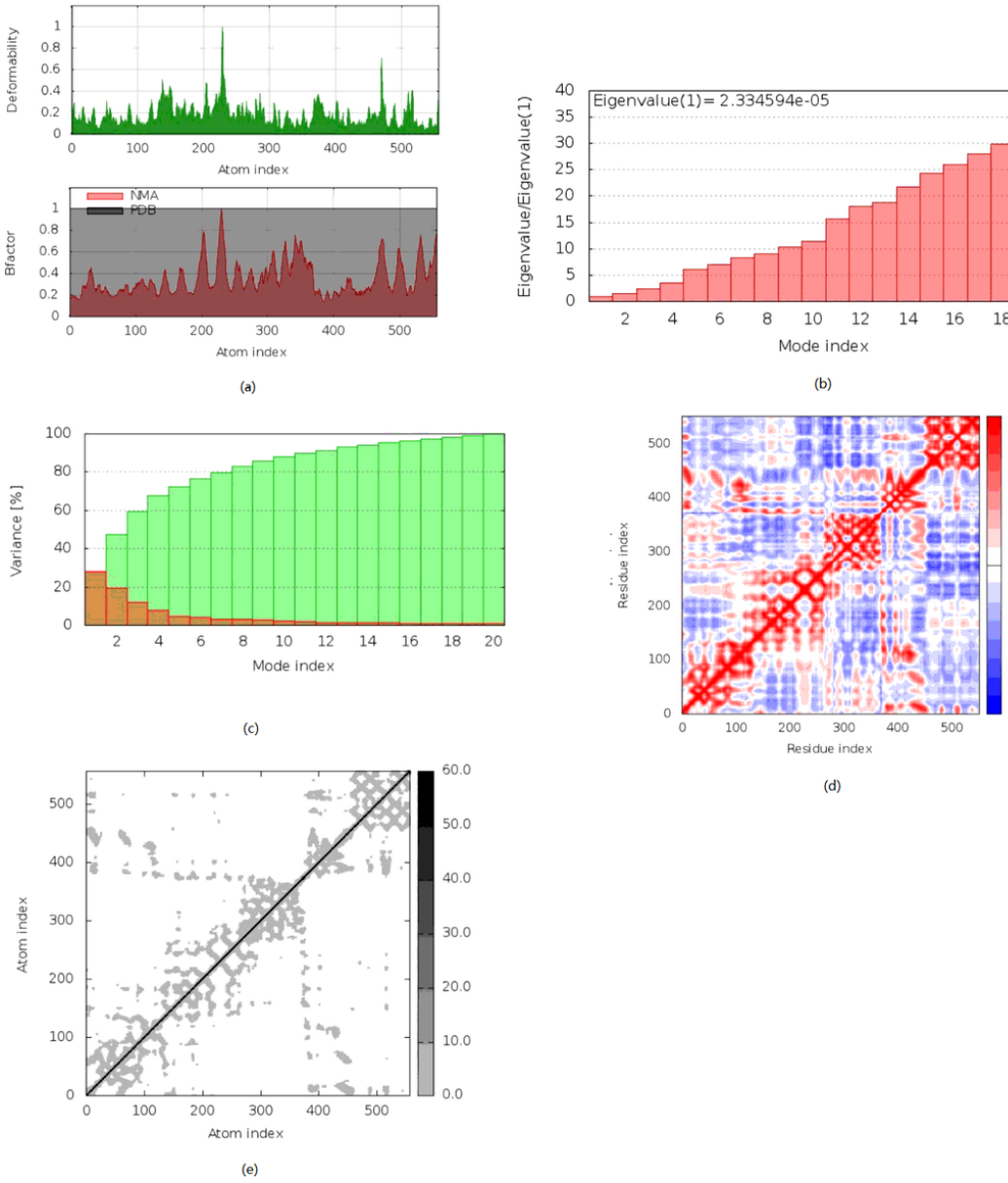

Figure 6

Molecular dynamic simulation of complex of vaccine 1 and HLA 1101, (a)Deformability and B-factor (b)Eigenvalues, the lower the eigenvalue, the easier the deformation. (c) Variance colored bars show the individual (red) and cumulative (green) variances. (d) Covariance map. (e) Elastic network.

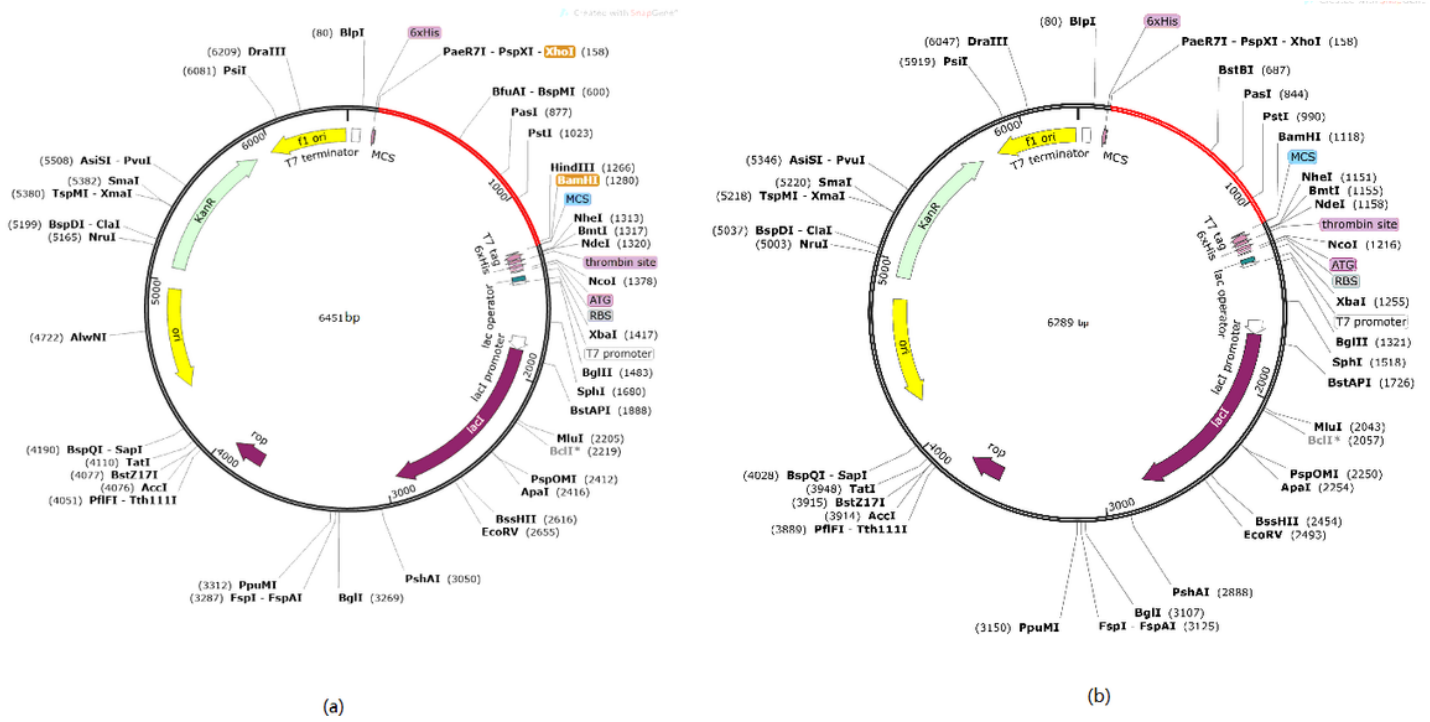

Figure 7

In silico cloning of codon-optimized vaccine into *E. coli* K12's expression system. The plasmid backbone is shown in black, while the inserted DNA sequence is shown in red. (a) Vaccine 1 (b)Vaccine 2.

Supplementary Files

This is a list of supplementary files associated with this preprint. Click to download.

- Supplementmaterial.docx